BOREAL ENVIRONMENT RESEARCH 5: 349–359 ISSN 1239-6095
Helsinki 20 December 2000

Using a cloud condensation nuclei counter to study CCN properties and concentrations

Pasi Aalto and Markku Kulmala

Department of Physics, P.O. Box 9 FIN-00014 University of Helsinki, Finland

Aalto, P. & Kulmala, M. 2000. Using a cloud condensation nuclei counter to study CCN properties and concentrations. *Boreal Env. Res.* 5: 349–359. ISSN 1239-6095

A Cloud Condensation Nuclei Counter (CCNC) has been constructed, calibrated and used in field conditions. The CCNC was used in a rural/boreal forest site (Hyytiälä), in marine/coastal sites (Tenerife and Mace Head), and in an urban site (Helsinki). Expressions for determining the soluble volume fraction of particles were derived. The soluble fraction of Aitken mode particles was determined and the CCNC number concentrations were observed. In the marine air masses the soluble fraction was seen to be around 0.8. In the rural site the soluble fraction was around 0.3 and some diurnal variation was seen. In Helsinki the soluble fraction was somewhat higher than in the boreal forest site.

Introduction

Atmospheric aerosol particles influence the Earth's radiation balance directly by scattering and absorbing solar radiation, and indirectly by acting as cloud condensation nuclei (CCN) (e.g. Charlson *et al.* 1992). While some progress has recently been made in evaluating the radiative effects of various aerosol components such as sulfate, organics, black carbon, sea-salt, and crustal species (Sokolik and Toon 1996, Kaufman and Fraser 1997, Winter and Chylek 1997, Chuang *et al.* 1997, Haywood and Ramaswamy 1998), substantial uncertainties still remain in the significance of both the direct and indirect radiative forcing. One of the key questions in reducing error bars is how aerosol particles grow to a CCN size and how they form cloud droplets. Once formed, clouds have a very extensive influence on the Earth's radiation budget through their albedo and greenhouse effects. In the future global warming, cloud properties may change due to the warmer and moister conditions, and possibly due to an increased aerosol particle load as well.

Clouds can affect electromagnetic radiation fluxes in the Earth's atmosphere by scattering and absorption. Locally the net effect is not very evident (e.g. because of different kind of surfaces) (*see* Curry 1995). According to measurements, however, the global net effect of today's clouds on the climate is probably cooling (*see* e.g. Hartmann and Doelling 1991) and thus opposite to the effect of greenhouse gases. The effects of clouds on the radiation fluxes depend on their depth, liquid water content, and cloud droplet size distribution (e.g. Twomey 1977).

The formation and growth of cloud droplets occur on pre-existing aerosol particles. Charac-

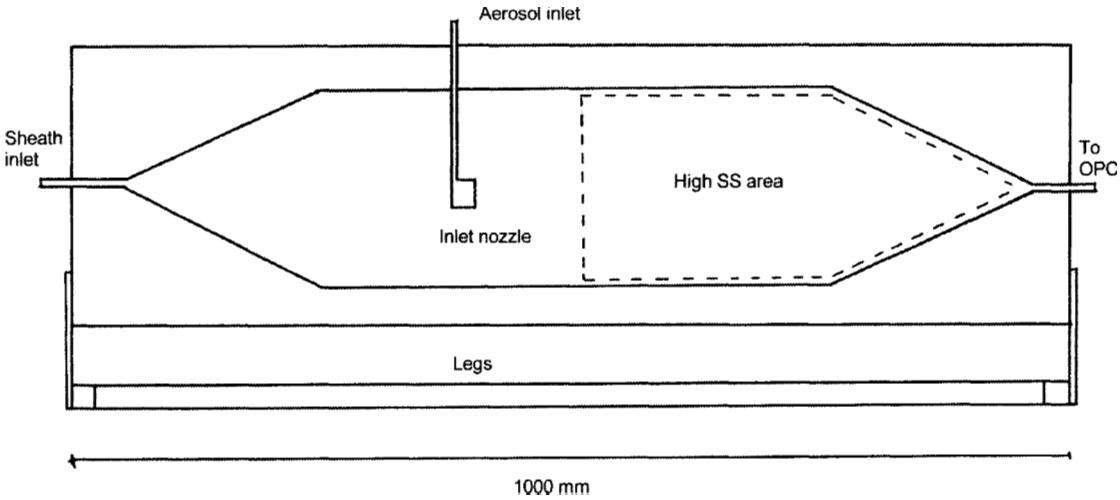

Fig. 1. Cloud condensation nuclei chamber from the side.

teristics such as the hygroscopicity of the pre-existing particle distribution strongly affect the developing cloud droplet distribution. Field experiments show that the pre-existing aerosol particle population is usually composed of mixed particles, i.e. particles including both hygroscopic and insoluble components (e.g. Svenningsson *et al.* 1992, 1994, Zhang *et al.* 1993). According to our recent model studies (Korhonen *et al.* 1996a, Kulmala *et al.* 1996), the soluble mass of pre-existing aerosol particles, together with their size distribution, is the most important factor (other than dynamics) in determining the developing cloud droplet distribution: Hygroscopic material decreases the saturation vapour pressure of water vapour above the surface of a solution droplet, which makes the formation of a cloud droplet easier. The condensation of different gaseous substances into aqueous particles during their growth increases the hygroscopicity of the particles. When the amount of the hyroscopic material in the particles increases, also the critical supersaturation needed for their activation to cloud droplets decreases (for further details *see* e.g. Kulmala *et al.* 1993, Korhonen *et al.* 1996b).

In order to understand the behaviour of CCN in the atmosphere, their concentrations and other properties should be measured as a function time. With a CCN counter it is possible to measure the concentration of aerosol particles able to act as CCN in the atmosphere (e.g. Twomey 1963, Laktionov 1972, Hudson and Squires 1976, Alofs 1978, Leaitch and Megaw 1982, Hudson 1989). These particles play an important role in the atmosphere because cloud droplets are formed on them. Typically cloud droplets are formed in the atmosphere when water supersaturation is between 0.1 and 1 percent. In the present study, we have developed a CCN counter, calibrated it, and used it in various conditions. We have also derived two simple formulas for evaluating the soluble mass fraction of CCNs.

Instrumentation

In order to analyze the CCN concentrations and the soluble fraction of aerosol particles, a cloud condensation nuclei counter (CCNC) was constructed and calibrated. This CCN counter is a modified version of the prototype (Aalto and Kulmala 1993).

The CCN counter is a thermal gradient diffusion cloud chamber with horizontal flow direction and two vertical parallel walls (Fig. 1). The total chamber length is one meter, the height is 20 cm, and the width is 16 mm. In this instrument the aerosol sample flows between two wetted, temperature-controlled walls. The walls are kept wet by attaching a filter paper on the walls of the chamber and keeping the water in the bottom in contact with the filter paper. Particle-free sheath air is fed into the chamber from one end of the chamber. Aerosols are fed into the centerline of the

chamber through an inlet nozzle. The high supersaturation area is about 40 cm long, giving a growth time of 20 seconds for particles. Stable supersaturation and temperature profiles are reached in a few seconds inside the chamber. When a small temperature difference is introduced between the walls, the saturation ratio between the plates will exceed unity. The chamber wall temperatures are controlled by heated baths. Typical supersaturations used with the chamber are between 0.2 and 1.0%. A 1% supersaturation is reached under normal conditions using a five-degree temperature difference between the walls (Brown and Schowengerdt 1979). The typical total flow rate through the chamber is three liters per minute (LPM), and the aerosol flow rate is 0.5 LPM. Droplets are counted after the chamber with an optical particle counter, Climet 7300 (OPC). Droplets larger than one micrometer in diameter are considered to be activated. With the supersaturations used in the instrument, this threshold diameter is good for discriminating between activated droplets and non-activated haze particles.

The measurement system contains an ordinary DMPS-system (Differential Mobility Particle Sizer), including a particle neutralizer, a Hauke-type differential mobility analyzer (DMA), and a particle counter (CPC). The CCN counter is used in parallel with the particle counter (Fig. 2). The instrument is typically calibrated using ammonium sulphate.

The system can be used in different configurations. In all configurations atmospheric aerosols are sampled with a constant flow rate, a monodisperse size fraction is selected from the total sample with the DMA, and the concentration of this fraction (CN) is measured with a CPC. The same sample is fed into the CCN counter, in which the water supersaturation is between 0.2% and 1.0%. The supersaturation can be selected to be any value between these two limits. Some fraction of the aerosol sample activates inside the chamber. The concentration of this activated fraction (CCN) is measured with an optical particle counter after the chamber. This concentration is compared with the total particle concentration, and the CCN/CN ratio is calculated. This is the primary data produced by the device. Since the DMA does not produce an exactly monodisperse aerosol because of the multiple charging of particles,

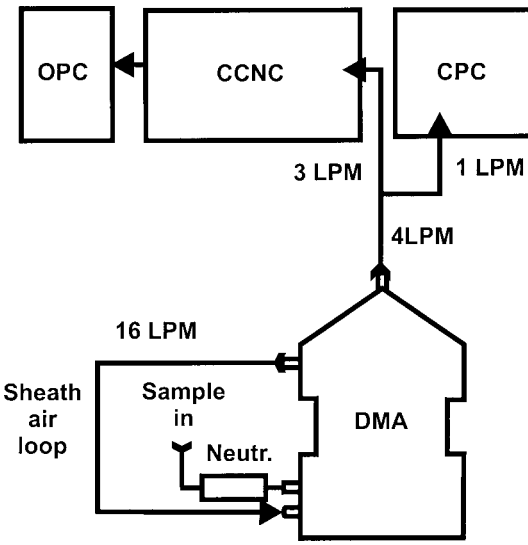

Fig. 2. The measurement system.

a direct analysis of the data does not give an exactly right value for the activated fraction. However, under normal conditions both the direct and the more detailed analysis give almost similar results. One can use the instrument in two configurations. The first is to set a supersaturation, to scan several sizes, and to determine how small particles are activated at this supersaturation. The second is to set a particle size and to scan different supersaturations to see the threshold supersaturation at which the particles are activated. In the theoretical section both these methods are analyzed.

Examples of calibrations with different configurations are presented in Figs. 3 and 4. The calibrations were done with ammonium sulphate particles. For a diameter scan with a constant 0.5% supersaturation (Fig. 3), the critical particle diameter is 43 nanometers. All particles larger than this size should be activated. Two things are obvious from the results. The activation curve does not increase sharply near the size of a critical diameter. This indicates that the supersaturation is not constant inside the chamber. This is true, since the supersaturation profile is parabolic between the chamber walls. Near the walls the supersaturation is zero and reaches its maximum near the centerline of the chamber. Although particles are fed along the centerline of the chamber, some mixing occurs which causes the particles to ex-

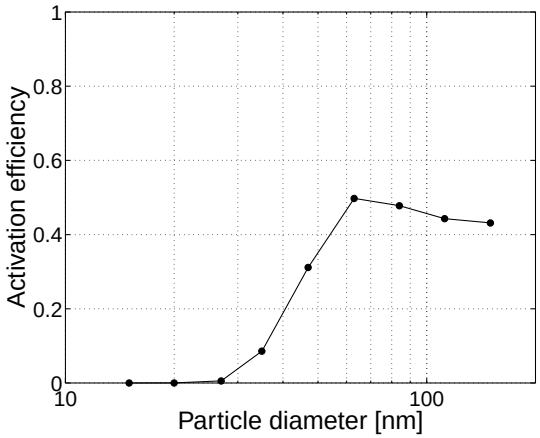

Fig. 3. Calibration with ammonium sulphate at 0.5% supersaturation.

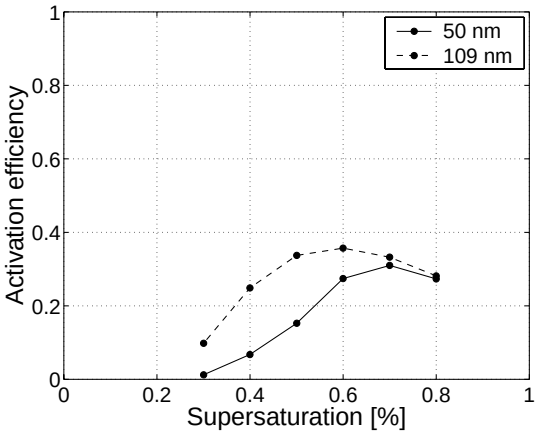

Fig. 4. Calibration with 50 nm and 109 nm ammonium sulphate particles with different supersaturations.

perience a range of supersaturations before they are counted with the OPC. The second problem is that the CCN/CN ratio does not reach unity. This indicates that there are some losses inside the chamber. This occurs partly because of droplet deposition before the OPC or inside the OPC, and partly because some of the particles never get activated because of mixing.

The second calibration example (Fig. 4) is a supersaturation scan with two different particle diameters. 50 nm particles should be activated at 0.4% supersaturation and 109 nm particles at 0.12% supersaturation. The same problem exists with this configuration as with the first one. From this calibration it can be seen that particle losses are a function of supersaturation. With this configuration the best detection efficiency is reached at 0.6% supersaturation. If the supersaturation is higher the droplets grow too large and are deposited, and if supersaturation is smaller they do not grow enough to be reliably detected with the OPC.

Estimations of the measurement errors can be made from the calibrations made during the campaigns. During a measurement campaign the instrument was typically calibrated once a day. During the Hyytiälä campaign, spring 1998, the mean value and the standard deviation for the CCN/CN ratio in the calibration data was 0.40 ± 0.06. For the critical diameter the mean and the standard deviation was 37 ± 3 nm. Frequent calibrations are really needed with this instrument. Unstable ambient aerosol concentration is making the situation even worse and because of that real error estimates are difficult to calculate. The high error estimates in the critical diameter also lead to high errors in the calculated soluble fractions. We have estimated that relative errors as high as 20% are possible.

Particle activation theory

The data obtained with the CCNC can be evaluated with the Köhler equation (*see* e.g. Seinfeld and Pandis 1998):

$$\ln(S) = \frac{A}{d} - \frac{B}{d^3 - d_i^3} \tag{1}$$

Here S is the saturation ratio, d is the droplet diameter and d_i is the diameter of an insoluble core. The terms A and B are

$$A = \frac{4M_w\sigma_w}{RT\rho_w} \tag{2}$$

$$B = \frac{6n_sM_w}{\pi\rho_w} = \frac{\nu\varepsilon_m d_s^3\rho_sM_w}{\rho_wM_s} \tag{3}$$

Here ν is the number of ions resulting from the dissociation of one soluble molecule. For example, $\nu = 2$ for NaCl and $NaNO_3$ and $\nu = 3$ for $(NH_4)_2SO_4$. ε_m is the mass fraction of the soluble material, ν_s is the number of moles of solute, d_s is the dry particle diameter, including soluble and

insoluble material, ρ_s is the density of soluble material, M_w is the molecular weight of water, M_s is the molecular weight of soluble material, σ_w is the surface tension of the droplet, T is droplet temperature, and R is the gas constant.

According the the traditional Köhler theory, aerosol particles will activate to cloud droplets when the saturation ratio is higher than the critical (activation) saturation ratio S_c given by

$$S_c = \exp\left(\sqrt{\frac{4A^3}{27B}}\right) \quad (4)$$

Although the traditional Köhler equation does not include all possible components present in the modified Köhler equation, such as soluble trace gases or slightly-soluble substances (Kulmala *et al.* 1997, Laaksonen *et al.* 1998), it includes two of the most important components, namely the soluble salt and the insoluble fraction. The modified Köhler curves and the traditional ones agree with each other in non-polluted conditions. Keeping in mind the accuracy of the instrument itself, and that most of measurements were performed in non-polluted conditions, the version of the Köhler expression given above is accurate enough for our data evaluation.

The activation threshold, or the saturation ratio, needed for the activation of a certain soluble aerosol like ammonium sulphate can be obtained from the Köhler theory. The calibrations was performed using the Köhler theory and activation was also observed.

Traditionally when using a CCNC, the number of CCN was measured at different fixed supersaturations. When a size-resolving CCNC (with DMA) was used, also the soluble fraction can be estimated with the Köhler equation. Therefore, it is an extension to the traditional use of a CCNC. We admit that a **T**andem **D**ifferential **M**obility **A**nalyzer (TDMA) is a better instrument for determining the soluble fraction. However, the CCNC is complementary to the TDMA because it gives the soluble fraction in supersaturated conditions, not at the 90% humidity at which TDMA measurements are customary made.

There are two ways to find out the soluble mass fraction. If an actual aerosol particle having a diameter d_a is activated at the same saturation as an ammonium sulphate particle (diameter d_s), then

$$\varepsilon_m = \frac{d_s^3}{d_a^3} \quad (5)$$

If the particle diameter is kept constant and the needed saturation ratio for activation is changed, then

$$\varepsilon_m = \left(\frac{\ln S_s}{\ln S_a}\right)^2 \quad (6)$$

Therefore, with the full capacity of the instrument, the mean solubility of different size particles can be determined, although Eq. 5 does not give the soluble fraction for any specific particle diameter but to some diameter around the activation threshold. However, with a CCNC it is not possible to obtain the solubility distribution that can typically be obtained with a TDMA.

Field applications of the CCN counter

The instrument was used in different field campaigns. The CCN number concentrations corresponding to different supersaturations and particle diameters were measured, and the soluble fractions of Aitken mode particles were determined. With the CCNC measurements and the particle size distribution data, it would be possible to calculate also the total CCN concentration at a given supersaturation. However, in this study we focused on the CCN properties, not their total concentrations.

The Hyytiälä site

The CCNC measurements were done in Hyytiälä during three extensive Biofor (Biogenic Aerosol Formation in the boreal forests) field campaigns in 1998 and 1999 (Kulmala *et al.* 2000).

Spring 1998 and summer 1998

During these periods the system was operated with a constant supersaturation and a variable particle diameter. The supersaturation was 0.5% and the particle diameter varied between 15 and 150 nm.

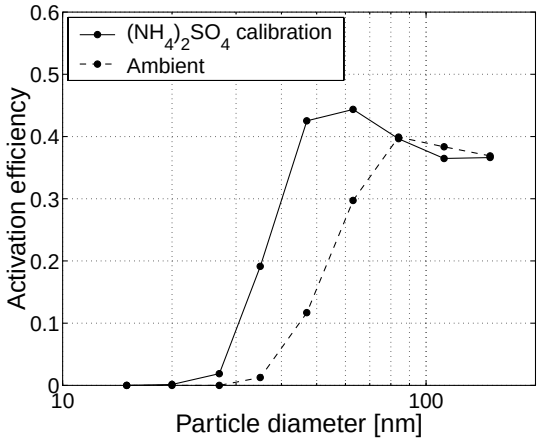

Fig. 5. Average calibration and ambient data during Biofor, spring 1998.

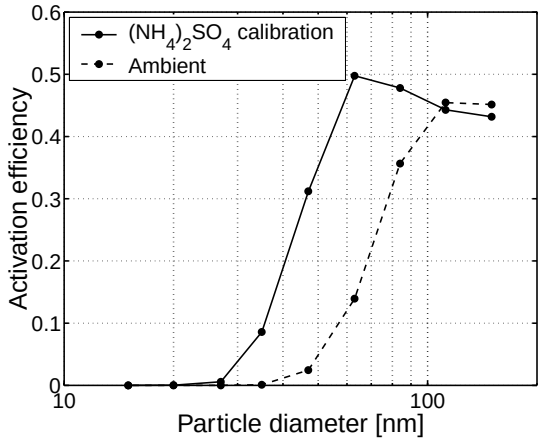

Fig. 6. Average calibration and ambient data during Biofor, summer 1998.

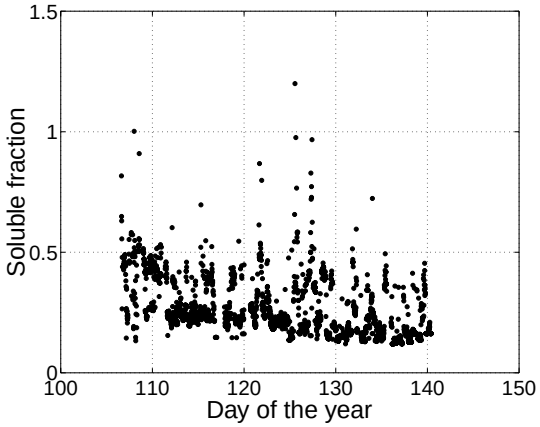

Fig. 7. Aerosol soluble fraction during Biofor, spring 1998.

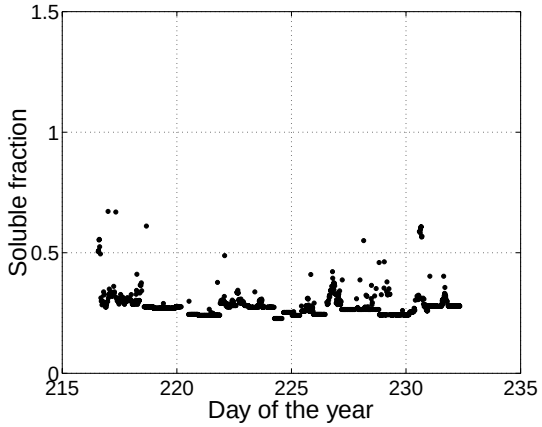

Fig. 8. Aerosol soluble fraction during Biofor, summer 1998.

The aerosol was sampled from a height of 18 meters above the forest. The sampling line length was 30 meters, the line diameter was 23.7 mm, and the flow rate was 25 LPM. According to the Köhler theory, ammonium sulphate particles should be activated at 0.5% supersaturation when their diameter is larger than 42 nm. It is evident from the calibration results that more than half of the particles were lost inside the CCN counter (Figs. 5 and 6). This fraction varied slightly between the spring and summer campaigns. During the spring about 40% of the particles were detected and during the summer almost 50%. The activation threshold value for ammonium sulphate was not exactly 42 nm as it should have been. During the spring the 50% cut size was around 35 nm and during the summer it was 42 nm.

If one takes into account the shift in the activation threshold, atmospheric aerosols seem to have been quite similar during the spring and summer campaigns (Figs. 5 and 6). During both campaigns, particles started to be activated when the particle diameter was around 70 nm.

The soluble mass fraction of Aitken mode particles calculated with Eq. 5 were mostly between 0.1 and 0.5 (Figs. 7 and 8). Variations during the summer campaign seemed to be very low. No significant diurnal variation was observed.

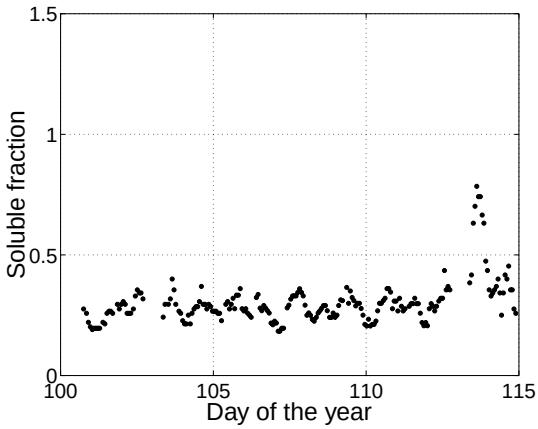

Fig. 9. Aerosol soluble fraction during Biofor, spring 1999. Particle diameter is 50 nm.

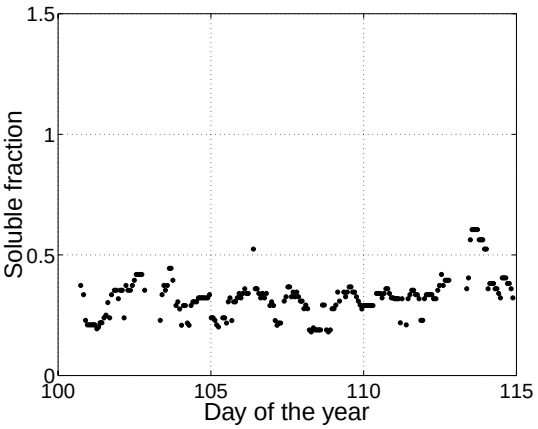

Fig. 10. Aerosol soluble fraction during Biofor, spring 1999. Particle diameter is 73 nm.

Spring 1999

During this period the system was at first operated in a same way as during the previous campaigns. At the beginning of April the system was re-configured so that three particle diameters were selected (50, 73 and 109 nm) and five supersaturations between 0.3% and 0.8% were scanned. The aerosol was sampled inside the forest. The sampling line was three meters long and four mm in diameter. The flow rate was 3.5 LPM. Fig. 4 shows the supersaturation scan with 50 nm and 109 nm ammonium sulphate particles. All 109 nm particles should be activated at all supersaturations. The 50 nm particles should start to be activated at 0.4% supersaturation. Instead of this, the supersaturation had to be around 0.5% to achieve half of the 109 nm curve value. It seems that the supersaturation was off from the predicted value.

The soluble fraction calculated with Eq. 6 was always found to be quite low. The minimum values found were around 0.2 and the maximum close to 0.4 (Figs. 9 and 10). Some diurnal variation was found in the solubility. The soluble fraction was on average 0.07 higher during the day than during the nighttime. The activation efficiency at 0.5% supersaturation was also lower at night than during the day. The solubilities calculated from the CCNC and the TDMA measurements were compared and a reasonably good agreement between them was found (K. Hämeri, M. Väkevä, P. Aalto, M. Kulmala, E. Swietlicki, W. Seidl, E. Becker & C. D. O'Dowd unpubl.).

Marine and coastal sites

The Tenerife measurements were made during the second Aerosol Characterization Experiment (ACE-2) in a lighthouse in Punta del Hidalgo, located directly on the shore line on the NE tip of Tenerife from June to July, 1997 (Raes *et al.* 2000). This was the first time when the CCNC was in use in the field. The sample was taken through a common aerosol inlet 63 meters above the sea level. Two supersaturations (0.2% and 0.5%) were used and four dry particle diameters were scanned (166, 73, 50, and 35 nm). This was the only time when the chamber was calibrated with NaCl particles. In calculating the soluble fraction, the calibration was shifted to the estimated ammonium sulphate calibration by adding 15 nm to the NaCl calibration diameters. This value comes from the Köhler theory. The air in Tenerife was mostly free from local pollution. Over ten days the measured air was affected by European plume outbreaks, the rest of the time it was clean marine air.

The soluble fraction was always quite high. The minimum values observed were around 0.6 and the maximum values close to unity (Fig. 11). The variability was quite high, and over some time

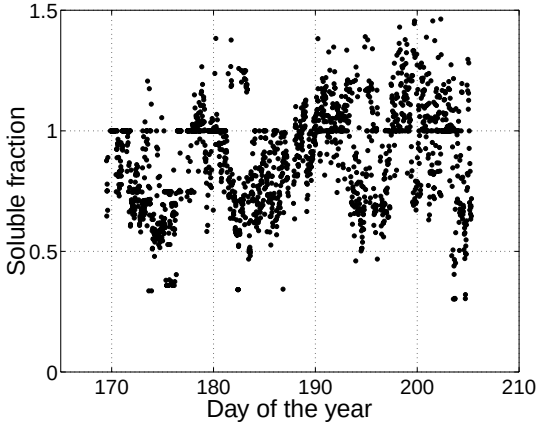

Fig. 11. Aerosol soluble fraction during ACE-2 calculated from 0.2% supersaturation measurements.

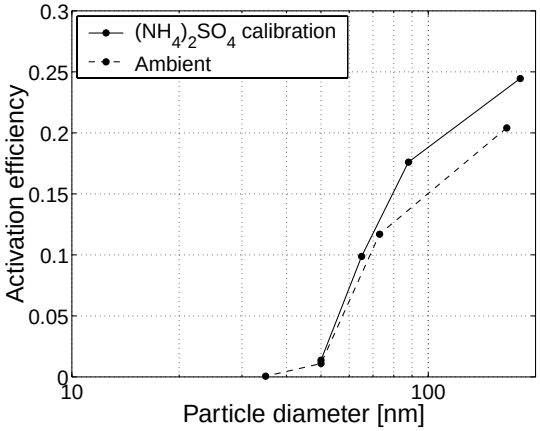

Fig. 12. Average calibration curve compared with the average measurement during ACE-2. The supersaturation is 0.2%.

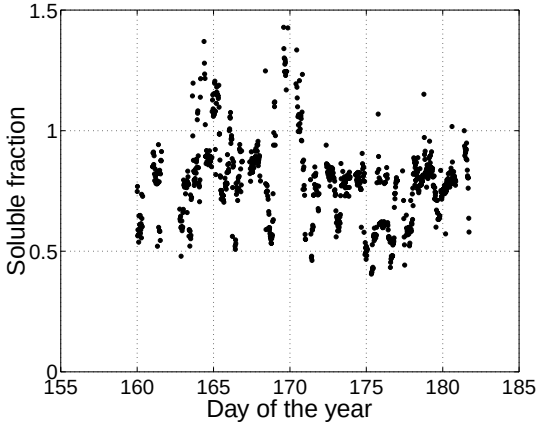

Fig. 13. Aerosol soluble fraction during the Parforce campaign calculated for 50 nm particle diameter.

intervals also values greater than unity were detected. These events might be partly due to the correction made for the calibration data to shift it from NaCl to ammonium sulphate, partly because the particles could have been more hygroscopic than ammonium sulphate particles. No diurnal variation was found. No difference between the clean marine air and the European outbreak situations was found. The average ambient spectrum quite closely resembled the $(NH_4)_2SO_4$ calibration (Fig. 12). Similar kinds of results were obtained from the TDMA measurements (Swietlicki *et al.* 2000).

The Mace Head measurements were made during two Parforce (Particle Formation and Fate in the Coastal Environment) campaigns at Mace Head, northwestern Ireland September 1998 and June 1999. The site is located directly on the shore line. The sample was taken through a common inlet ten meters above the sea level. The site on Mace Head was also marine, but local pollution was more common than in Tenerife. During the first campaign, one supersaturation of 0.5% was used and nine diameters (150, 112, 84, 63, 47, 35, 27, 20, and 15 nm) were scanned. During the second campaign six supersaturations (0.3%, 0.4%, 0.5%, 0.6%, 0.7% and 0.8%) were scanned with two dry particle diameters (109 and 50 nm).

The conditions at Mace Head were quite similar to those in Tenerife. The soluble fraction was quite high during clean marine air periods. When local pollution was present the soluble fraction fell to 0.4 (Fig. 13). In Fig. 14, the average calibration curve is compared against average ambient measurement. At Mace Head the ambient activation efficiency differed more from its calibrated value than in Tenerife. No clear diurnal variation was observed.

Urban site

Measurements in Helsinki were made during the Sytty (Finnish Research Programme on Environmental Health) campaign, January 1999, downtown of Helsinki. The closest main streets were just a few hundred meters from the location. One

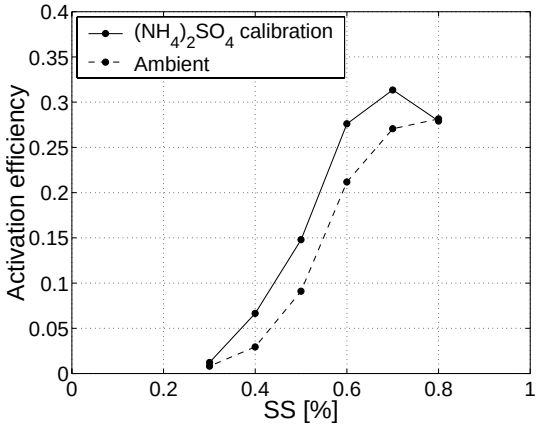

Fig. 14. Average calibration curve compared with the average measurement during Parforce. Particle diameter is 50 nm.

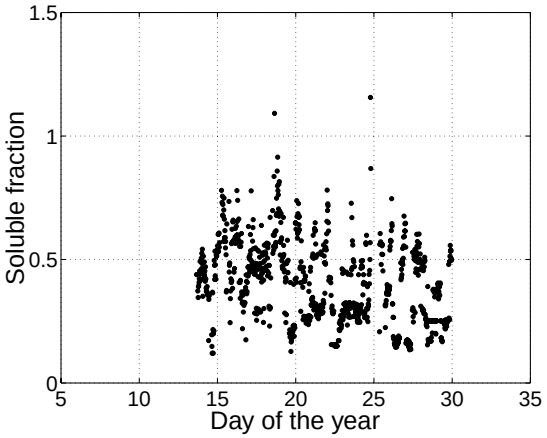

Fig. 15. Aerosol soluble fraction during Sytty studies in Helsinki calculated from 0.5% supersaturation measurements.

supersaturation of 0.5% was used and ten diameters (150, 117, 90, 70, 54, 42, 32, 25, 19, and 15 nm) were scanned.

In the downtown area the soluble fractions were quite similar to those in Hyytiälä. The typical values were around 0.3 (Fig. 15). Some diurnal variation was detected in the activation efficiency. During the day the efficiency was on average 0.1 units smaller than during the night, indicating that during daytime externally mixed particles of low solubility appeared. This is quite understandable, since during daytime the aerosol number was dominated by emissions from traffic. Most of the high-soluble-fraction incidents occurred during the nighttime. The average spectrum shows quite a small activation efficiency compared to the calibration (Fig. 16). Compared to the Hyytiälä measurements the ambient spectrum grew more slowly to larger sizes. During the measurements the variable ambient aerosol concentration often interfered with the measurements.

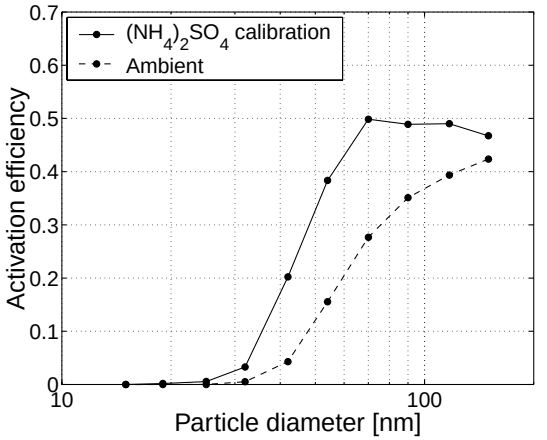

Fig. 16. Average calibration curve compared with the average measurement during Sytty measurements in Helsinki. The supersaturation is 0.5%.

Comparison of different sites

The mean activated fraction at 0.5% supersaturation for three particle diameters and soluble fractions at different sites are presented in Table 1. On the marine sites both the soluble fraction and the activated fraction were high. In Helsinki the variation of the soluble fraction was quite large, and the activated fractions were lower than in other sites. In Hyytiälä, the soluble fraction was lower than in Helsinki, but the activated fraction was higher.

Conclusions

A cloud condensation nuclei counter (CCNC) has been designed, constructed, calibrated and tested. The cloud condensation nuclei were measured during all Biofor and PARFORCE campaigns. In addition to this, the CCNC was also used during the ACE2 HILLCLOUD campaign and in an ur-

Table 1. Overview of the different sites.

Site	Soluble fraction	Activated fraction,SS = 0.5%		
		50 nm	73 nm	109 nm
Tenerife, summer 1997	0.9 ± 0.2	0.7	1.0	1.0
Ireland, summer 1999	0.8 ± 0.2	0.6	–	1.0
Hyytiälä, spring 1998	0.26 ± 0.12	0.35	0.8	1.0
Hyytiälä, summer 1998	0.28 ± 0.05	0.15	0.5	1.0
Hyytiälä, spring 1999	0.32 ± 0.08	0.35	0.8	1.0
Helsinki, winter 1999	0.4 ± 0.2	0.35	0.6	0.8

ban area in Helsinki. In the present paper, a method to estimate the soluble volume fraction in aerosol particles has been derived and used to investigate the soluble fraction of Aitken mode particles.

In the marine air masses the soluble fraction was found to be around 0.8. In the rural site, the soluble fraction was found to be around 0.3 with some diurnal variation. In Helsinki, the soluble fraction was somewhat higher than in the boreal forest site, but larger particles were activated less efficiently in Helsinki than in the boreal forest site in Hyytiälä.

The CCNC data seems to be reasonably reliable, but showing some variations that can be taken into account in the further analysis. The data can be used together with the particle size distribution data to calculate the total concentration of cloud condensation nuclei and to estimate the hygroscopic properties of aerosols. The hygroscopicity can be analyzed in more detail with TDMA measurements and with aerosol chemical analyses.

ACKNOWLEDGEMENTS: The authors would like to acknowledge financial support from the Academy of Finland. We would also like to thank Toivo Pohja for constructing the chamber. During field studies the instrument has been maintained by many people. The authors especially wish to thank Minna Väkevä, Ismo Koponen, Jyrki Mäkelä, Kaarle Hämeri, Olle Berg and Erik Swietlicki.

References

Aalto P. & Kulmala M. 1993. Building of a laminar flow diffusion chamber for the study of cloud condensation nuclei. *Report Series in Aerosol Science* 23: 199–203.

Alofs D.J. 1978. Performance of a Dual-Range Cloud Nucleus Counter. *J. App. Met.* 17: 1286–1297.

Brown J.T.Jr. & Schowengerdt F.D. 1979. Analysis of a continous flow parallel plate thermal diffusion cloud chamber. *J. Aerosol Sci.* 10: 339–348.

Charlson R.J., Schwartz S.E., Hales J.M., Cess R.D., Coakley J.A.Jr., Hansen J.E. & Hofmann D.J. 1992. Climate forcing by anthropogenic aerosols. *Science* 255: 423–430.

Chuang C.C., Penner J.E., Taylor K.E., Grossman A.S. & Walton J.J. 1997. An assessment of the radiative effects of anthropogenic sulfate. *J. Geophys. Res.* 102: 3761–3778.

Curry J.A. 1995. Interactions among aerosols, clouds and climate of the Artic Ocean. *The Science of the Total Environment* 160/161: 777–791.

Hartmann D.L. & Doelling D. 1991. On the net radiative effectiveness of clouds. *J. Geophys. Res.* 96: 869–891.

Haywood J.M. & Ramaswamy V. 1998. Global sensitivity studies of the direct radiative forcing due to anthropogenic sulfate and black carbon aerosols. *J. Geophys. Res.* 103: 6043–6058.

Hudson J.G & Squires P. 1976. An Improved Continuous Flow Diffusion Cloud Chamber. *Journal of Applied Meteorology* 15: 776–782

Hudson J.G. 1989. An Instantaneous CCN spectrometer. *Journal of Atmospheric and Oceanic Technology* 6: 1055–1065.

Kaufman Y.J. & Fraser R.S. 1997. The effect of smoke particles on clouds and climate forcing. *Science* 277: 1636–1639.

Korhonen P., Kulmala M., Hansson H.-C., Svenningsson I.B. & Rusko N. 1996a. Hygroscopicity of pre-existing particle distribution and formation of cloud droplets: A model study. *Atmospheric Research* 41: 249–266.

Korhonen P., Kulmala M. & Vesala T. 1996b. Model simulation of the amount of soluble mass during cloud droplet formation. *Atmos. Environ.* 30: 1773–1785.

Kulmala M., Laaksonen A., Korhonen P., Vesala T., Ahonen T. & Barrett J.C. 1993. The effect of atmospheric nitric acid vapour on cloud condensation nucleus activation. *J. Geophys. Res.* 98: 22949–22958.

Kulmala M., Korhonen P., Vesala T., Hansson H.-C., Noone

K. & Svenningsson B. 1996. The effect of hygroscopicity on cloud droplet formation. *Tellus* 48B: 347–360.

Kulmala M., Laaksonen A., Charlson R.J. & Korhonen P. 1997. Cloud without supersaturation. *Nature* 388: 336–337.

Kulmala M., Hämeri K., Mäkelä J.M., Aalto P.P., Pirjola L., Väkevä M., Nilsson E.D., Koponen I.K., Buzorius G., Keronen P., Rannik Ü., Laakso L., Vesala T., Bigg K., Seidl W., Forkel R., Hoffmann T., Spanke J., Jansson R., Shimmo M., Hansson H.-C., O'Dowd C., Becker E., Paatero J., Teinilä K., Hillamo R., Viisanen Y., Laaksonen A., Swietlicki E., Saalm J., Hari P. & Altimir N 2000. Biogenic aerosol formation in the boreal forest. *Boreal Env. Res.* **5: XX–XX**.

Laaksonen A., Korhonen P., Kulmala M. & Charlson R.J. 1998. Modification of the Köhler Equation to Include Soluble Trace Gases and Slightly Soluble Substances. *J. Atmos. Sci.* 55: 853–862.

Laktionov A.G. 1972. A Constant Temperature Method of determining the Concentrations of Cloud Condensation Nuclei. *Izv. Atmospheric and Oceanic Physics* 8: 672–677.

Leaitch R. & Megaw W.J. 1982. The diffusion tube: a Cloud Condensation Nucleus Counter for use below 0.3% supersaturation. *J. Aerosol Sci.* 13: 297–319.

Raes F., Bates T., McGovern F. & Van Liedekerke M. 2000. The 2nd aerosol characterization experiment (ACE-2): general overview and main results. *Tellus* 52B: 111–125.

Seinfeld J.H. & Pandis S.N. 1998. *Atmospheric chemistry and physics: from air pollution to climate change*, A Wiley-Interscience publication, USA, 1326 pp.

Sokolik I.N. & Toon O.B. 1996. Direct radiative forcing by anthropogenic airborne mineral aerosols. *Nature* 381: 681–683.

Svenningsson I.B., Hansson H.-C. Wiedensohler A., Ogren J.A., Noone K.J. & Hallberg A. 1992. Hygroscopic growth of aerosol particles in the Po-valley. *Tellus* 44B: 556–569.

Svenningsson I.B., Hansson H.-C. Wiedensohler A., Noone K.J., Ogren J., Hallberg A. & Colvile R. 1994. Hygroscopic growth of aerosol particles and its influence on nucleation scavenging in cloud: experimental results from Kleiner Feldberg. *J. Atmos. Chem.* 19: 129–152.

Swietlicki E., Zhou J., Covert D.S., Hämeri K., Busch B., Väkevä M., Dusek U., Berg O.H., Wiedensohler A., Aalto P., Mäkelä J., Martinsson B.G., Papaspiropulos G., Mentes, B., Frank G. & Sratmann F. 2000. Hygroscopic prperties of aerosol particles in the north-eastern Atlantic during ACE-2. *Tellus* 52B: 201–227.

Twomey S. 1963. Measurements of natural cloud nuclei. *Journal de Recherches Atmosphiriques* 1: 101–105

Twomey S. 1977. The influence of pollution on the shortwave albedo of clouds. *J. Atmos. Sci.* 34: 1149–1152.

Winter B. & Chylek P. 1997. Contribution of sea salt aerosol to the planetary clear-sky albedo. *Tellus* 49B: 72–79.

Zhang X.Q., McMurry P.H., Hering S.V. & Casuccio G.S. 1993. Mixing characteristics and water content of submicron aerosols measured in Los Angles and at the Grand Canyon. *Atmos. Environ.* 27A: 1593–1608.

Received & March 2000, accepted 17 August 2000